

Malaria Early Warning Application for Individual Risk Assessment

Sagar Sadak^{1†}, Cayden Goeringer^{2†}, Janiah Kyle^{3†}

*For correspondence:

sadaksagar9@gmail.com,
caydengoeringer@gmail.com,
janiah.kyle@gmail.com ()

†These authors contributed equally to this work

¹School of Computing and Augmented Intelligence, Arizona State University, Tempe, Arizona, USA; ²School of Life Sciences, Arizona State University, Tempe, Arizona, USA; ³Spelman College, Atlanta, Georgia, USA

Abstract As one of the oldest known diseases to inflict humanity (since the Agricultural Revolution about 12,000 years ago), malaria has proven to be a significant global challenge. Many intervention strategies have been undertaken in the last few decades such as widespread ITN/LLIN and IRS use and yet even with great success, malaria continues to be a ravaging disease requiring inventive solutions. In this study, a malaria early warning system is developed which utilizes an adapted Ross-MacDonald model to assess individual risk and disease epidemiology. Strategies for achieving a disease-free equilibrium state are also shown by performing local asymptotic stability analysis. The stages of the mosquito life cycle are highly influenced by weather conditions, both in the aquatic and adult stages, as well as the use of insecticides (either through ITN/LLIN use or via IRS), therefore, we consider regional data parameters, such as weather conditions, parasite rate and resistance, to estimate deviated risk from the baseline, with the final product being a progressive web application (i.e. a mobile app). Such a product has widespread application primarily in holoendemic areas in Africa to inform both native and tourist populations of their relative risk.

Introduction

Malaria is mainly a tropical disease caused by the parasitic *Plasmodium*, transmitted via the bite of infected female *Anopheles* mosquitoes. Although

it is preventable and curable, it was responsible for 241 million cases and 627,000 deaths in 2020 alone [1]. The continent of Africa, specifically the western and central regions, are most affected by this disease, accounting for around 95% of the cases and 96% of the deaths while a vast majority of these deaths (~80%) occur in children under the age of 5 [1].

Plasmodium are a species of sexually-reproducing eukaryotic protozoans, whose life-cycle involves the affliction of two hosts, an invertebrate host (e.g. mosquitoes) that serves as a vector for transmission and a site for sexual reproduction, and a vertebrate host (e.g. reptiles, rodents, primates) where asexual reproduction and sexual development occurs, leading to the disease we know as malaria [12].

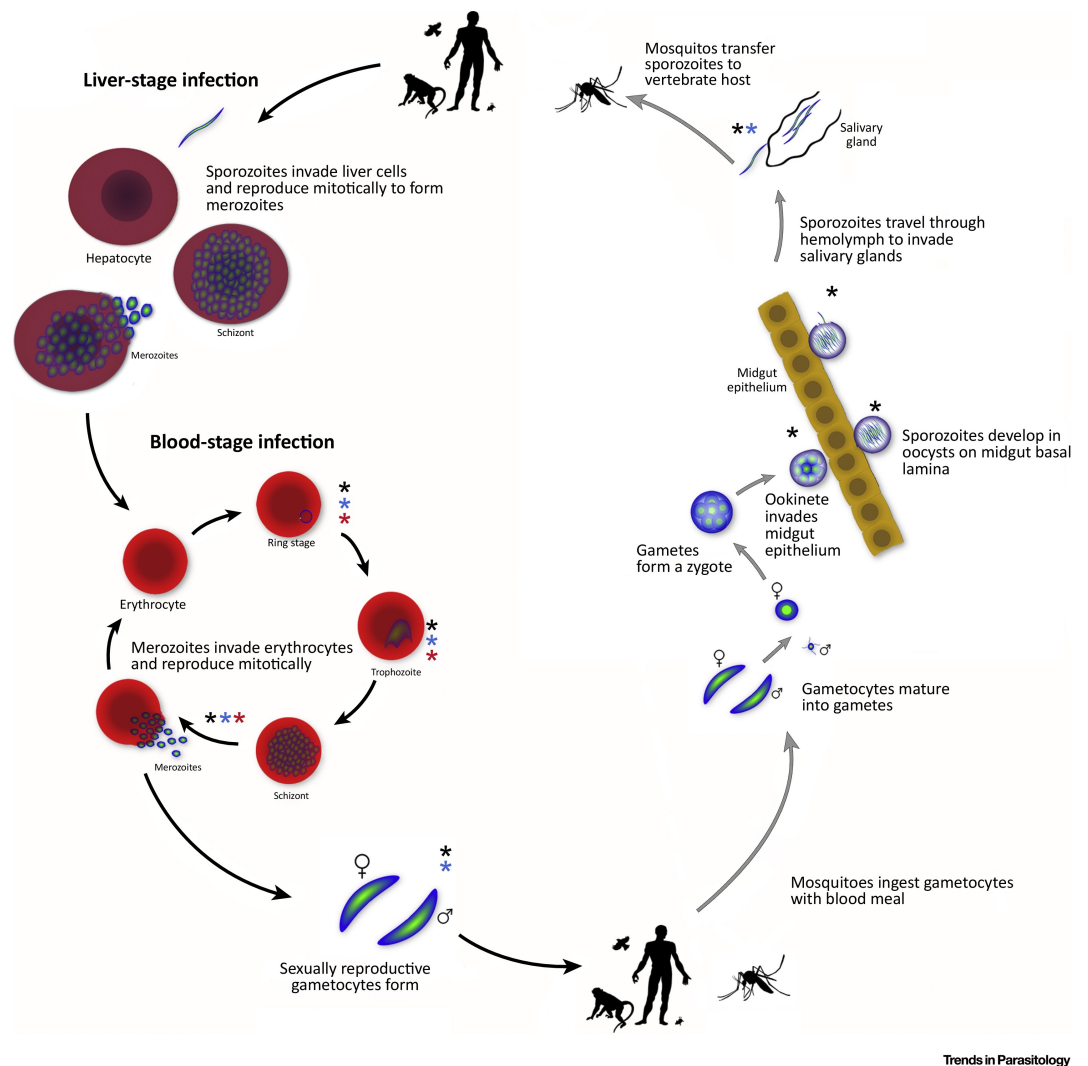


Figure 1. Lifecycle of *Plasmodium*, following its transmission and development in the invertebrate and vertebrate hosts. Image sourced from Figure 1 from [12].

The disease being transmitted by mosquitoes first originated by a protozoan which adapted to live in the gut of aquatic invertebrates and where in the midgut lumen, the exogenous sexual phase of gamete formation and fertilization takes place, known as sporogony [2]. This process has been well summarized [14] and condensed as follows. When the disease enters the mosquito after taking a blood meal, the gametocytes initiate the sporogonic cycle in the midgut forming microgametocytes and macrogametocytes that fuse to form a zygote [20]. The zygote transforms into a ookinete that moves through the mosquito gut lining and transforms into an oocyst which produces sporozoites that are released after the oocyst bursts. The sporozoites then travel to infect the salivary glands that become infectious to humans.

Of the five species of *Plasmodium* that affect humans, two are most notable: *P. falciparum* and *P. vivax*, with *P. falciparum* being most prevalent in sub-Saharan Africa, and therefore being the primary focus of this study.

It has been hypothesized that approximately 10,000 years ago following The Last Glacial Period, rapid warming of the planet into the Holocene Epoch created the beginnings of agricultural practices that maintained suitable conditions for malaria to evolve through creation of anopheline habitats from changes in land use [2][15]. Humans become involved following a successful infectious mosquito bite where the inoculation process is initiated by sporozoites traveling into the parenchymal cells of the liver, the site of parasite development. The start of this phase in the liver named schizogony, in which the sporozoites replicate, resulting in a tissue schizont that contains thousands of merozoites [3]. Following maturation, the schizont containing the infected hepatocytes ruptures and releases merozoites that invade erythrocytes in a cyclic bursting process where trophozoites feed to become new merozoites that infect more erythrocytes [3]. Eventually, the environmental conditions will initiate the transformation of a few haploid asexual-stage parasites into gametocytes that circulate in the peripheral bloodstream that when taken up by a feeding female mosquito will transmit the disease [20].

The lifecycle of an Anopheles mosquito, consisting of the immature and adult stages, is highly dependent on weather conditions (such as temperature and precipitation). The variability in these conditions results in different prevalence levels of malaria for different locations. This is attributed to the fact that mosquitoes favor relatively warm tropical climate,

stagnant water bodies, and a sufficient population of hosts to acquire a blood meal (for the egg development process). Compounding to these factors that mosquitoes prefer, the broader socio-economic background of residents, land-use practices, as well as the level of development of the area (including sanitation infrastructure and the availability of medical care), all affect the level of malaria prevalence and subsequently, its risk of contraction for any particular location. This idea is the backbone of the application; local variability is used to assess risk in relation to the annual baseline.

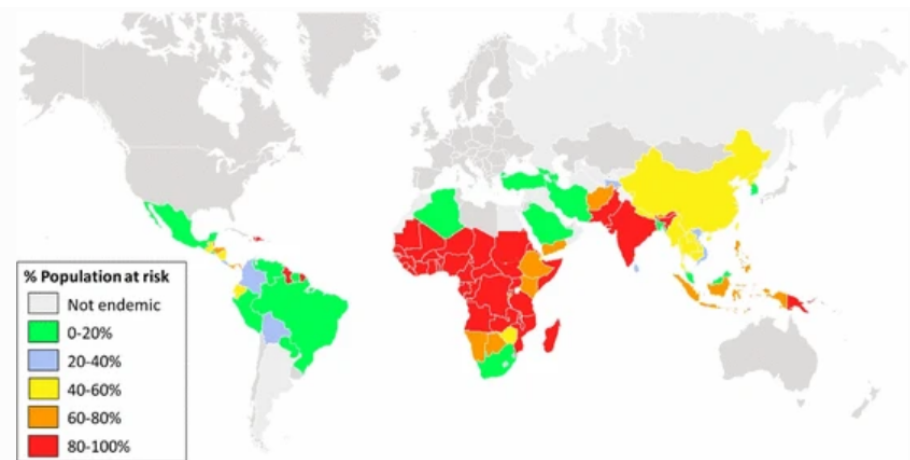


Figure 2. Percentage of population at risk of malaria in 2013. As shown, most of the risk is concentrated in Africa and south-southeast Asia. Image sourced from Figure 1 from [14]

With nearly half the world's population at risk of this disease, its eradication has been of primary concern to various organizations around the world, such as the World Health Organization (WHO), the Bill and Melinda Gates Foundation, and the US President's Malaria Initiative. [1]. The socio-economic impact and development of many countries is greatly afflicted by malaria which has been proven since as early as 1965 to cause much lower economic growth and where reductions in malaria are associated with much higher economic growth [4]. Although significant steps have been taken towards its eradication by a multitude of such groups, it is nevertheless a leading cause of death in many developing countries, thus warranting immediate global cooperative action [6]. A key tool in malaria prevention has been the insecticide-treated nets (ITNs) and long-lasting

insecticidal nets (LLINs) with their great success evident by the distribution of 2 billion nets supplied to sub-Saharan Africa between 2004-2020 [1]. The use of ITNs have proven to be useful for prevention and even reducing childhood mortality [5]. In recent years, however, growing resistance of the mosquitoes to insecticides has rendered many pyrethroid chemicals (and thus, ITNs and LLINs) less effective [14]. Nearly all across Africa, resistance has been observed to some extent and even across different vector groups due to many different evolved mechanisms including knockdown resistance [23].

Since ITNs and LLINs alone are not sufficient for eradicating malaria, a combination of preventive measures is currently the best course of action. Therefore, we developed a malaria early warning system (MEWS) as a mobile application and website to warn users of their risk of contracting malaria in a specific region. The goal is that it serves as a site for the spread of reliable, life-saving information regarding malaria, as well as to inspire behavioral changes in people whether it be through advising the use of bed nets or to stay away from stagnant water bodies servicing as mosquito breeding spots. The MEWS will be an important component in the fight against malaria as it provides real time information to general public about potential risk in order to prevent additional cases.

Previous works for a malaria early warning system (MEWS) have had similar, but not identical, ideas and methods as this paper. An online MEWS recognizes the effects rainfall has on transmission and focuses on creating an early warning system for rain so one can then predict the risk of contracting malaria [27]. However, the risk itself is not calculated, or at least not blatantly stated, by the system itself. In addition, most of the graphs presented focus only on rainfall and require interpretation, making the experience less user friendly than our MEWS. Another online MEWS provides more detailed information: Vulnerability, Seasonal Climate Forecasts, Monitoring the Environment and Observed Malaria Morbidity [28]. However, this can only be accessed as a website, not a mobile application. The novelty in our MEWS is that it is accessible through the web or as a mobile application and is user-friendly.

The MEWS will first obtain the user's current location or the location he/she will travel to in the future, then obtain relevant data, such as temperature, to evaluate potential infections and the user's individual risk. For this to happen, the MEWS requires mathematical modeling that can be evaluated at any given time. Thus, the mathematical model consists

mostly of differential equations.

The model used in this study has a long history traced back to the first models of malaria from Ronald Ross written in the early 1900s that were advanced in the following decades by those such as Alfred J. Lotka and George Macdonald to more accurately capture the disease properties of malaria [18]. From the progression of these mathematical models came new ideas including entomological inoculation rate, basic reproduction number, and vectorial capacity which addressed the need to assess transmission and epidemiology [18]. More recent advancements have improved the accuracy of past models by including properties related to immunity and climate that improve modeling accuracy. The epidemiology of malaria since Macdonald also highlighted the importance of endemicity when observing populations with malaria highlighting the requirements that should be met for potential eradication which despite being implemented ultimately failed [18].

A crucial component of modeling malaria is considering the role of weather on mosquito population dynamics. The early work of Lysenko and Semashko [19] which made initial discoveries of the temperatures required to sustain transmission and thus being influential for malarial endemicity which even at the time highlighted malaria global maximums nearer to the equator [15]. Although other weather factors such as rainfall and humidity contribute to malaria abundance, the role of temperature is especially important given that *Plasmodium falciparum* can maintain growth cycles until temperatures drop below 20°C [22].

Mathematical Models

In order to calculate the risk of contracting malaria in a particular region, dynamic mathematical models must be developed for both humans and mosquitoes. The human model and mosquito model are SEIR and SEI models respectively. For the mosquito dynamics, it is important to include both the adult stage and the immature/aquatic stage since both stages depend on one another. Only adult mosquitoes bite for blood meals, thus only adult mosquitoes dynamics are an SEI model. The immature mosquitoes will determine how many adult mosquitoes there will be. Therefore, the immature dynamics are an important factor in analyzing malaria transmission. Since humans have the ability to recover from malaria, the human dynamics are an SEIR model. Both the entomological inoculation rate (EIR) and the reproduction number of the disease (R_0) are

helpful in determining the risk on contracting malaria, however, this paper only considers EIR.

Immature/Aquatic Mosquito Dynamics

The mosquito immature/aquatic stage is comprised of 6 classes: the egg class, 4 larva classes, and the pupa class. For simplicity, this model combines all 4 larva classes into one class, thus having a total of 3 differential equations to represent the immature/aquatic stage of mosquitoes. The equations are described below:

$$\dot{E} = EFD(T) \left(1 - \frac{E}{K_E(R)} \right) N_m - \sigma_E(T)E - \mu_E(T)E$$

$$\dot{L} = \sigma_E(T)E - \sigma_L(T)L - \mu_L(T)L$$

$$\dot{P} = \sigma_L(T)L - q\sigma_P(T)P - \mu_P(T)P$$

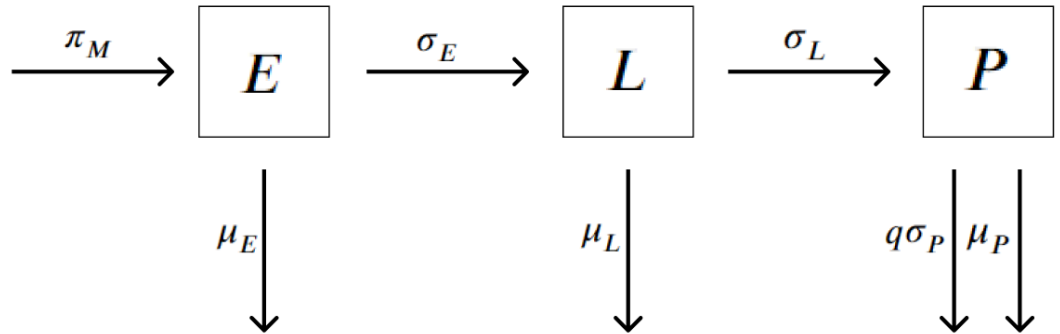


Figure 3. A graphic flowchart that illustrates the Aquatic stage dynamic model. The π_M term substitutes $EFD\left(1 - \frac{E}{K_E}\right)(N_m)$.

\dot{E} , \dot{L} , and \dot{P} are the change in the number of eggs, larva, and pupae over time respectively. $EFD(T)$ is the number of eggs laid per female mosquito per day [9]. To obtain the remaining proportion of potential eggs that can be laid in the future, the proportion of current eggs, E , to egg carrying capacity, $K_E(R)$, is subtracted from 1. The total number of mosquitoes, N_m , is then multiplied by the product of the number eggs laid per female

mosquito per day, $EFD(T)$, and the proportion of potential eggs that can be laid in the future, $\left(1 - \frac{E}{K_E(R)}\right)$. It is necessary to subtract eggs that develop into larva or die from this equation (See Table 2 for the descriptions of each parameter). The larva class receives immature mosquitoes that survived the egg class and loses larva that either progress to the pupa class or die off. The pupa class goes through a similar process with consideration that the proportion that are female, q , are the only type of mosquitoes we want to observe for the adult class. The formula for carrying capacity is adapted from White et al. [21] which was modeled as a convolution of recent rainfall with some weighting function which had been included as either a constant, linearly decreasing, or exponentially decreasing function. The constant weighting function was used here for simplicity which is:

$$K(t) = \lambda \frac{1}{\tau} \int_{t-\tau}^t \text{rain}(t') dt'$$

Where $\text{rain}(t)$ is daily rainfall and λ is the fitted scaling factor unique to the population data.

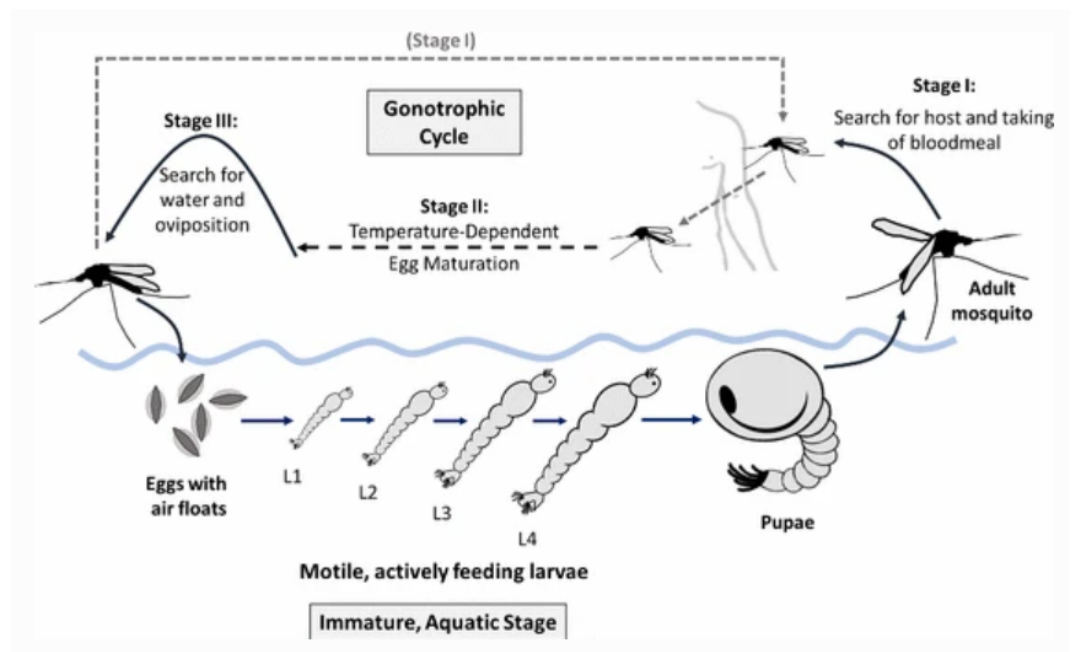


Figure 4. Stages of Mosquito development from egg to mature adult. Please note that the four instar stages (L1 to L4) have been combined into a single stage in our model. Image sourced from Figure 3 from [14].

Adult Mosquito Dynamics (sensitive to insecticides)

After surviving the immature stage, female mosquitoes develop into adults, seek hosts for blood, and, thus, are susceptible to malaria. A female mosquito that bites an infectious human moves from the susceptible class to the exposed class. A mosquito that becomes infectious at a rate σ_m move from the exposed class to the infectious class. Mosquitoes that die at the natural death rate μ_{ms} or die from contact of insecticide treated bed nets (ITNs) at a rate $\epsilon_B C_B \delta_B$ leave every class. The equations are written below.

$$\begin{aligned} \dot{S}_{ms} &= q\sigma_P(T)(1-f)P - \frac{\beta_{Hms} I_H S_{ms}}{N_H} - (\mu_{ms} + \epsilon_B C_B \delta_B) S_{ms} \\ \dot{E}_{ms} &= \frac{\beta_{Hms} I_H S_{ms}}{N_H} - \sigma_{ms} E_{ms} - (\mu_{ms} + \epsilon_B C_B \delta_B) E_{ms} \\ \dot{I}_{ms} &= \sigma_{ms} E_{ms} - (\mu_{ms} + \epsilon_B C_B \delta_B) I_{ms} \end{aligned}$$

It is important to note that the expression $(1-f)$ represents the proportion of female mosquitoes sensitive to an ITN compared to those resistant to insecticide.

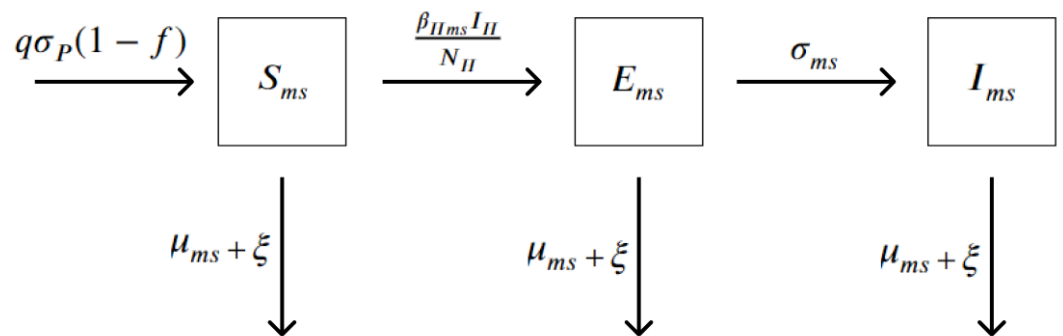


Figure 5. A graphic flowchart that illustrates the sensitive adult mosquito dynamic model. The ξ term substitutes $\epsilon_B C_B \delta_B$.

Adult Mosquito Dynamics (resistant to insecticides)

Similar to the adult mosquitoes sensitive to ITNs, the dynamics for the adult mosquitoes resistant to ITNs are written below:

$$\begin{aligned} \dot{S}_{mr} &= q\sigma_P(T)fP - \frac{\beta_{Hmr}I_H S_{mr}}{N_H} - (\mu_{mr} + \epsilon_B C_B \delta_B (1-u)) S_{mr} \\ \dot{E}_{mr} &= \frac{\beta_{Hmr}I_H S_{mr}}{N_H} - \sigma_{mr} E_{mr} - (\mu_{mr} + \epsilon_B C_B \delta_B (1-u)) E_{mr} \\ \dot{I}_{mr} &= \sigma_{mr} E_{mr} - (\mu_{mr} + \epsilon_B C_B \delta_B (1-u)) I_{mr} \end{aligned}$$

Note that f is used instead of $(1-f)$ to differentiate between resistant and sensitive mosquitoes, while the expression $(1-u)$ is used to differentiate the killing rates due of insecticide (δ_B) [17]. For simplicity, let the value of $\sigma_{ms} = \sigma_{mr} = \sigma_m$ (See Table 4)

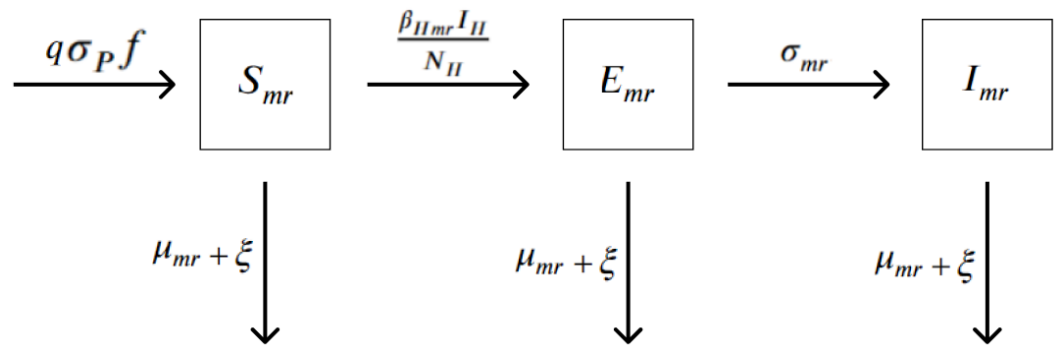


Figure 6. A graphic flowchart that illustrates the resistant adult mosquito dynamic model. The ξ term substitutes $\epsilon_B C_B \delta_B (1-u)$.

Human Dynamics

In a region where malaria is prevalent, humans become susceptible as soon as they are born or when they migrate to that particular region. In the human dynamic model, this is the recruitment rate, π_H . A human bitten by an infectious mosquito (resistant or susceptible to insecticide) moves from the susceptible class to the exposed class. In the model below, bed net efficacy, ϵ_B , and bed net coverage, C_B , are considered to determine the probability of transmission when bed nets are being used. The human dynamic model is described below.

$$\dot{S}_H = \pi_H - (1 - \epsilon_B C_B) \left(\frac{\beta_{msH} I_{ms}}{N_H} S_H + \frac{\beta_{mrH} I_{mr}}{N_H} S_H \right) - \mu_H S_H + \Psi_H R_H$$

$$\dot{E}_H = (1 - \epsilon_B C_B) \left(\frac{\beta_{msH} I_{ms}}{N_H} S_H + \frac{\beta_{mrH} I_{mr}}{N_H} S_H \right) - \mu_H E_H - \sigma_H E_H$$

$$\dot{I}_H = \sigma_H E_H - \gamma_H I_H - \mu_H I_H - \delta_H I_H$$

$$\dot{R}_H = \gamma_H I_H - \mu_H R_H - \Psi_H R_H$$

Let μ_h be the natural death rate for humans and let σ_H be the rate at which humans become infectious. The parameter r is the rate at which humans recover. Since immunity from malaria is only temporary, γ is the rate at which humans from the recovered class move back into the susceptible class. It should be considered that malarial superinfection and waning immunity complicates the most accurate model representation of immunity, especially in holoendemic populations where complete susceptibility renewal rarely occurs. Dynamics of recurring infection has been considered in recent models [9].

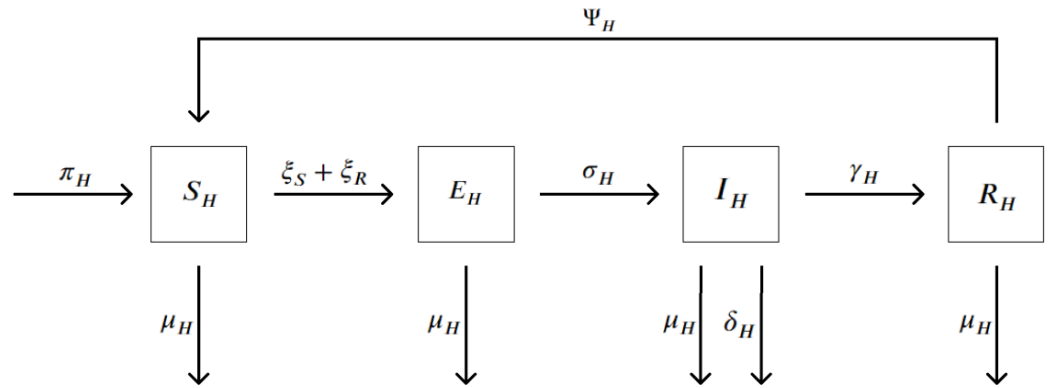


Figure 7. A graphic flowchart that illustrates the human dynamic model. The ξ_S and ξ_R terms substitute $(1 - \epsilon_B C_B) \left(\frac{\beta_{msH} I_{ms}}{N_H} \right)$ and $(1 - \epsilon_B C_B) \left(\frac{\beta_{mrH} I_{mr}}{N_H} \right)$, respectively.

Table 1. Description of State Variables

Variables	Interpretation
E	Number of eggs
L	Number of larvae (combination of all 4 instar stages)
P	Number of pupae
S_{ms}	Number of susceptible mosquitoes that are sensitive to insecticides
E_{ms}	Number of exposed mosquitoes that are sensitive to insecticides
I_{ms}	Number of infectious mosquitoes that are sensitive to insecticides
S_{mr}	Number of susceptible mosquitoes that are resistant to insecticides
E_{mr}	Number of exposed mosquitoes that are resistant to insecticides
I_{mr}	Number of infectious mosquitoes that are resistant to insecticides
S_H	Number of susceptible humans
E_H	Number of exposed (infected but not infectious) humans
I_H	Number of infectious humans
R_H	Number of recovered humans

Table 2. Description of Parameters

Parameters	Interpretation
$EFD(T)$	Eggs per female mosquito per day
$K_E(R)$	Carrying capacity of eggs
q	Proportion of female mosquitoes
N_m	Total number of mosquitoes
$\sigma_E(T)$	Development rate of eggs to larvae
$\mu_E(T)$	Natural death rate of eggs
$\sigma_L(T)$	Development rate of larvae to pupae
$\mu_L(T)$	Natural death rate of larvae
$\sigma_P(T)$	Development rate of pupae to adult
$\mu_P(T)$	Natural death rate of pupae
f	Proportion of resistant mosquitoes
β_{HM}	Transmission probability from infected human to a susceptible mosquito
μ_{ms}	Natural death rate of susceptible mosquitoes that are sensitive to insecticides
ϵ_B	Efficacy of bed nets
C_B	Coverage of bed nets
δ_B	Bed net-induced mortality rate
σ_{ms}	Development rate of mosquitoes that are sensitive to insecticides from exposed to infectious
μ_{mr}	Natural death rate of susceptible mosquitoes that are resistant to insecticides
u	Decrease in mortality rate of resistant mosquitoes in comparison to sensitive mosquitoes
σ_{mr}	Development rate of mosquitoes that are resistant to insecticides from exposed to infectious
π_H	Recruitment rate of humans
β_{msH}/β_{mrH}	Transmission probability from infected mosquito (that is sensitive to insecticides/resistant to insecticides) to a susceptible human
β_{Hms}/β_{Hmr}	Transmission probability from infected human to a susceptible mosquito (that is sensitive to insecticides/resistant to insecticides)

μ_H	Natural death rate of humans
Ψ_H	Rate of immunity loss of humans
σ_H	Development rate of humans from exposed to infectious class (Corresponds to time taken for <i>Plasmodium</i> to complete its schizogonic cycle)
r_H	Recovery rate of humans from malaria
δ_H	Death rate of humans from malaria
N_H	Total number of humans

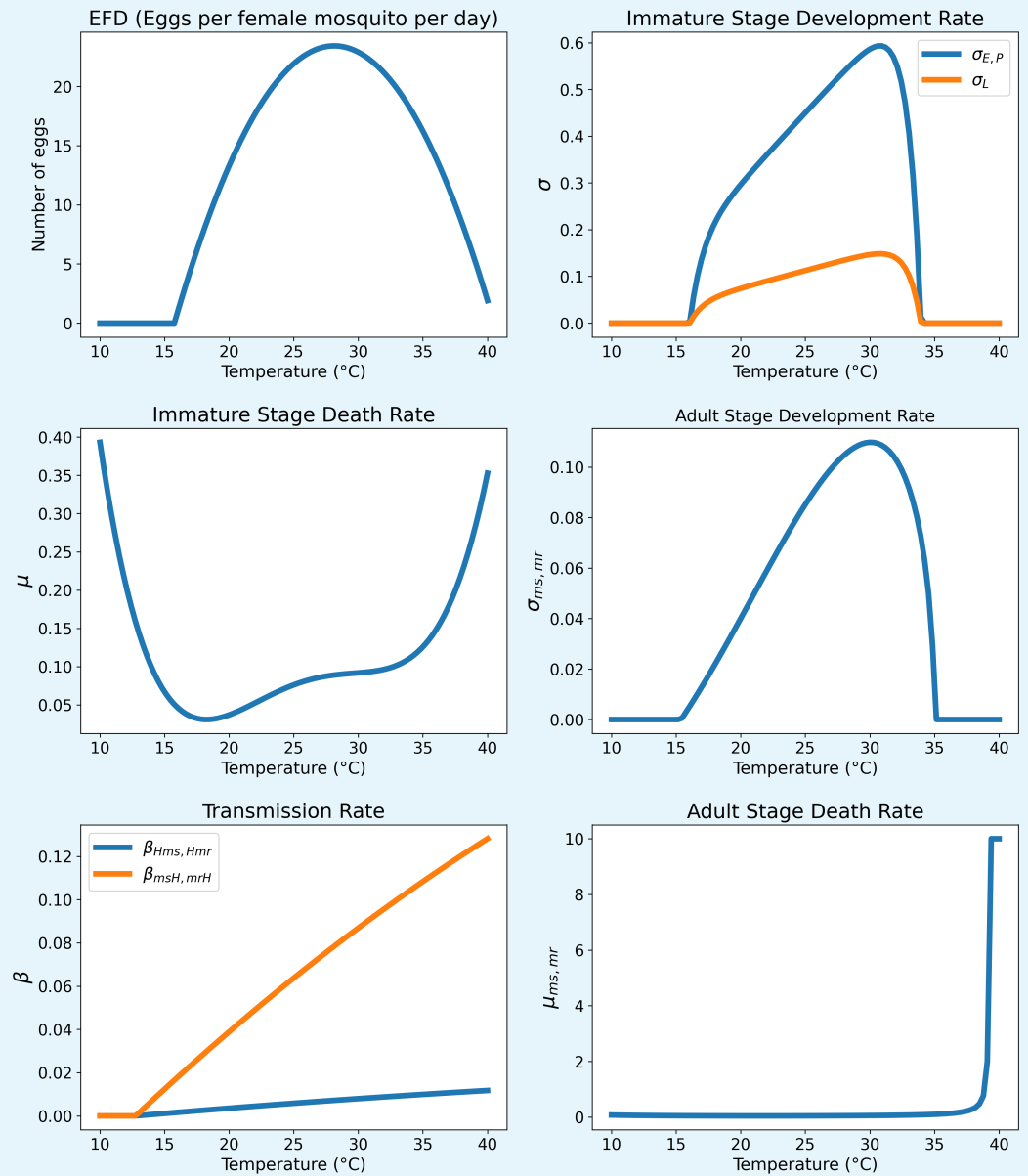
Table 3. Values for Parameters

Parameters	Baseline Values	Reference
q	0.5 (dimensionless)	[26]
f	0.1 (dimensionless)	Assumed
u	0.95 (dimensionless)	[7]
π_H	2.19 (per day)	[7]
r_H	1/30 (per day)	[10]
Ψ_H	0.0056 (per day)	[17]
σ_H	$\left(\frac{(12)(3.04)}{365}\right)$ (per day)	[9]
μ_H	0.00004 (per day)	[9]

Table 4. Functions for Dependent Parameters

Parameters	Functions	Reference
EFD(T)	$\max(0, -0.153T^2 + 8.61T - 97.7)$	[9]
$\sigma_{E,P}(T)$	$\max(0, 6(-0.05 + 0.005T - 2.139 \times 10^{-16}e^T - 281357.656e^{-T}))$	[10]
$\sigma_L(T)$	$\max(0, \frac{6}{4}(-0.05 + 0.005T - 2.139 \times 10^{-16}e^T - 281357.656e^{-T}))$	[10]
$\mu_{E,L,P}(T)$	$8.929 \times 10^{-6}T^4 - 9.271 \times 10^{-4}T^3 + 3.536 \times 10^{-2}T^2 - 0.5814T + 3.509$	[10]
$\beta_{Hms,Hmr}(T)$	$\max(0, 0.022(-0.00014T^2 + 0.027T - 0.322))$	[9]
$\beta_{msH,mrH}(T)$	$\max(0, 0.24(-0.00014T^2 + 0.027T - 0.322))$	[9]
σ_m	$\max(0, 0.000112T(T - 15.384)(\sqrt{35 - T}))$	[10]
$\mu_{ms,mr}$	$\left(\frac{1}{\max(0.1, -11.8239 + 3.3292T - 0.0771T^2)}\right)$	[10]

Box 1. Temperature Dependent Parameters



Box 1—figure 1. The figures above show the temperature-related dynamics of the model parameters, for which the equations are listed in the aforementioned table.

2.5 EIR

The entomological inoculation rate (EIR) gives the rate of infectious bites per unit time (generally per day) per person. In the application, EIR is the main metric used to determine risk. The equation is described below:

$$EIR = \beta(1 - \epsilon_B c_B) \left(\frac{I_{ms} + I_{mr}}{N_H} \right)$$

The EIR is defined as the product of the rate of transmission (considering the effect of bed net usage) and the proportion of infectious mosquitoes to humans [9]. The proportion of infectious mosquitoes to humans is defined as the total number of infectious mosquitoes (both resistant and sensitive) over the total number of humans.

3. Progressive Web Application (Mobile App)

There have been many advances in the multi-decade global effort to eradicate malaria. The use of bed nets, better living conditions, destruction of breeding sites, and more have proved to be effective in the decades past. However, insecticide resistance, among other issues, pose the next big obstacle to malaria eradication by 2040, one of United Nation's goals.

Therefore, in response to these issues and as a culmination to this research paper, a web/mobile application has been developed using various technologies, including Python, JavaScript, HTML, and CSS.

3.1 Data

Data is a major part of the app; acquiring and processing it posed one of the biggest issues during this study. To ensure a reliable risk approximation, we had to get data from multiple different sources, including locally saved datasets as well as APIs (Application programming interface). Listed below are some of them.

3.1.1 Weather

Temperature and precipitation have significant impacts on mosquito dynamics as many previous papers have studied [32][33]. Temperature affects nearly every single parameter in the aquatic and adult stages, whereas precipitation mainly influences the carrying capacity (K_E) of the eggs, which in turn has ripple effects that leads to changes in populations of mosquitoes as well as humans. Since the model was run for a time range of 365 days

before the present day, we used decadal monthly average temperature and precipitation data from WorldClim (<https://www.worldclim.org/>) as an estimate for weather conditions until 7 days before the present day. For the last week of the model run, more accurate data is sourced from the WeatherAPI (<https://www.weatherapi.com/>) (Please note that accurate historical weather for more than one week can be accessed through the API with a paid subscription). The rainfall data is used to estimate rainwater accumulation in a specific region, in order to understand the existence of conditions favorable for the laying and development of mosquito eggs. Accumulation is calculated using the equation below, where τ represents the rate of loss of accumulated water (via evaporation or ground absorption). The value used for τ in our model is 7, signifying that it takes about 7 days, on average, for accumulated rainwater to disappear.

$$\dot{R} = \text{rain}(t) - \left(\frac{1}{\tau}\right) R$$

The result is two arrays of length 365 consisting of temperature and rainwater accumulation data, respectively. As such, for each run of the model, these conditions are updated, and used to inform the parameter values, as described earlier in the paper.

3.1.2 Insecticide Resistance

The use of ITN/LLINs and IRS brought about huge success in combating malaria, vastly reducing the number of cases and deaths [1][34]. Unfortunately, however, this success turned out to be a double-edged sword. Alongside saving millions of lives, it also led to widespread resistance in mosquitoes, thus rendering the very tools that were effective a while ago, almost useless. This growing concern is one of the influences for this study and the development of this product. Until stronger insecticides are created or newer methods for fighting malaria are found, this app is expected to help ensure that populations, not only those local to Africa but also foreign tourists, are aware of the present risk of malaria in their respective regions.

Below is a graphical illustration of the data used in the app. It factors in percent mortality reduction of mosquitoes from various different insecticides for any given location, based on latitude-longitude coordinates. The data, called IRMapper (<https://anopheles.irmapper.com/>), itself is produced by a joint initiative of Vestergaard, KEMRI-CGHR and ESRI Eastern Africa.

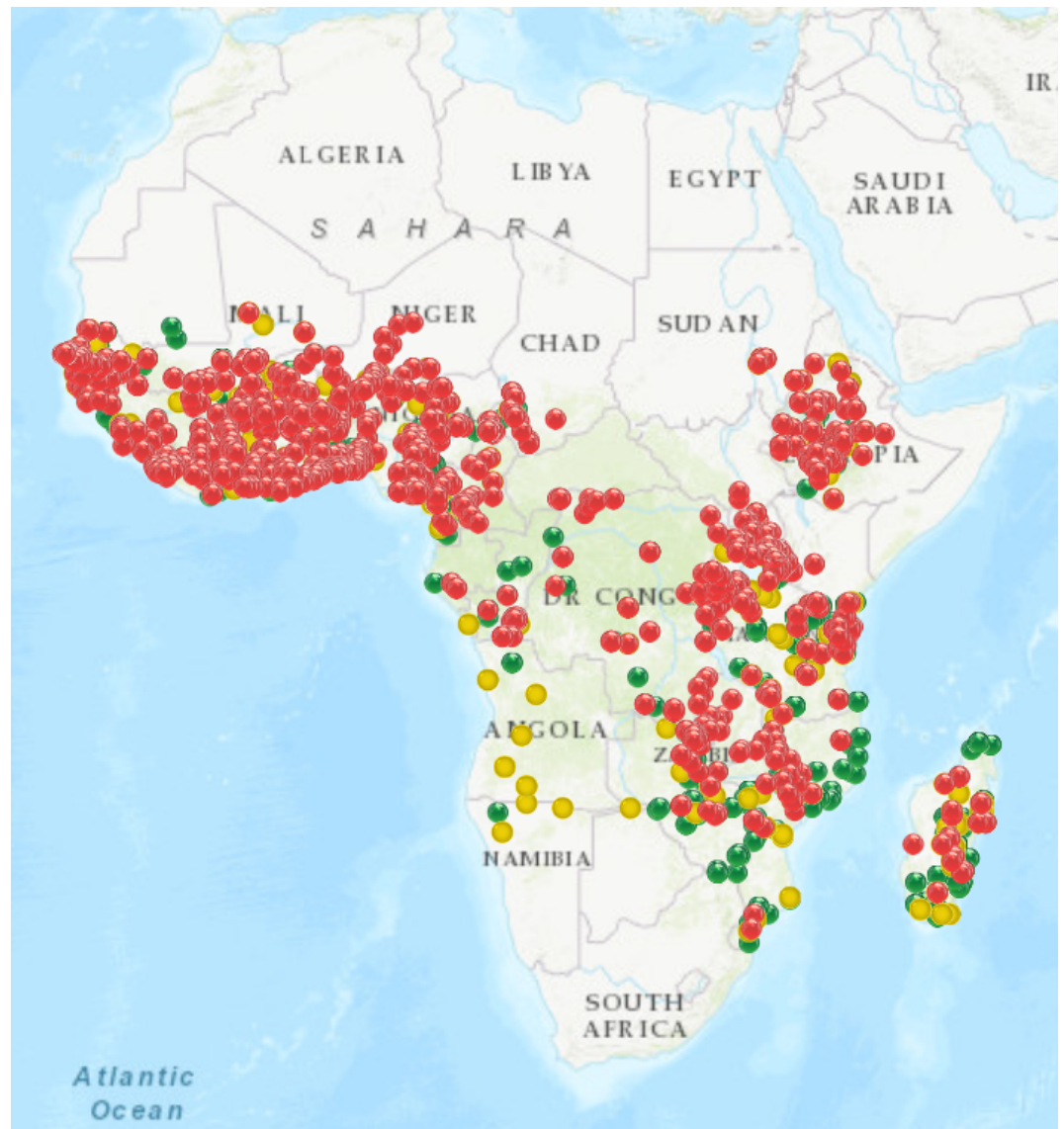


Figure 8. The map above shows the resistance of *Anopheles* mosquitoes to pyrethroids (the primary chemical in ITNs and LLINs). Red: Confirmed resistance; Yellow: Possible resistance; Green: Sensitive. Image sourced from the IRMapper [16].

3.1.3 Malaria Prevalence and Mortality

Knowing the demographic information for the user's location can allow us to accurately set the initial values for the state variables, i.e., S_H , I_H , etc. As such, a raster image is sourced from WorldPop (<https://hub.worldpop.org/doi/10.5258/SOTON/WP00004>), which consists of pixel-wise population data, with a resolution of 0.00833333 decimal degrees or approximately 1 kilometer.

This population data is coupled with the parasite rate raster image from the Malaria Atlas Project (<https://malariaatlas.org/malaria-burden-data-download/>) to, in turn, acquire the estimated number of infected humans (I_H) to begin running the model. As expected, highly endemic areas will have higher parasite rates, thus leading to higher estimates of EIR once the model is finished running. The Malaria Atlas Project is also the source of malaria-related human mortality data, corresponding to the parameter δ_H in our model.

3.1.4 Bed Net Usage

A present-day malaria model would not be an accurate representation of reality if it did not incorporate bed net usage and its effect on the mortality of mosquitoes for sensitive and resistant classes appropriately. The Malaria Atlas Project website hosts a research project (<https://malariaatlas.org/research-project/metrics-of-insecticide-treated-nets-distribution/>) that was conducted to gather this information, which was graciously made available for open access, thus enabling us to use it freely.

4. Results

4.1 Mathematical Proofs and Theorems

4.1.1 Basic Qualitative Properties

The model monitors the temporal dynamics of mosquito populations, all the state variables and parameters are non-negative. The parameters related to natural mortality at each life-stage and the environmental carrying capacity are positive and finite. Similarly the grouping and process for bounding from [29] and [26] is closely followed. The state variables are grouped by life-cycle stage, organism, and adult insecticide resistance status, let:

$$\begin{aligned} \mathcal{B}_1 &= (S_H, E_H, I_H, R_H), \mathcal{B}_2 = (S_{ms}, E_{ms}, I_{ms}), \\ \mathcal{B}_3 &= (S_{mr}, E_{mr}, I_{mr}), \mathcal{B}_4 = (E_m, L_m, P_m). \end{aligned}$$

Definition 1

Following [26], for the time-dependent parameters the following quanti-

ties hold:

$$a^* = \sup_{t \geq 0} a(t) \quad a_* = \inf_{t \geq 0} a(t)$$

For the immature mosquito groups, since $(1 - (E/K_E))_+ \geq 0$, then $E(t) \leq K_E$ for all t . Thus, using Definition 1, it can be deduced from the immature mosquito compartments using the larval stage described in the model that (where a dot represents differentiation with respect to time t),

$$\dot{L} = \sigma_E(T)E - [\sigma_L(T) + \mu_L(T)]L \leq \sigma_E^* K_E - (\sigma_L^* + \mu_L^*)L$$

So that following by the Gronwall inequality:

$$\limsup_{t \rightarrow \infty} L(t) \leq \frac{\sigma_E^* K_E}{\sigma_L^* + \mu_L^*} = L^\diamond$$

With the bounds from above in the equations, it is similarly found that:

$$\limsup_{t \rightarrow \infty} P(t) \leq \frac{\sigma_L^* L^\diamond}{\sigma_P^* + \mu_P^*} = P^\diamond$$

Using the above equation, furthermore it can be shown for adult mosquito groups:

$$\dot{N}_{ms} = \sigma_P(T)(1 - f)P - (\mu_{ms}(t) + \epsilon_B C_B \delta_B)N_{ms} \leq \sigma_P^*(1 - f)P^\diamond - (\mu_{ms}^* + \epsilon_B C_B \delta_B)N_{ms}$$

$$\text{from which it follows } \limsup_{t \rightarrow \infty} N_{ms}(t) \leq \frac{\sigma_P^*(1-f)P^\diamond}{\mu_{ms}^* + \epsilon_B C_B \delta_B} = N_{ms}^\diamond$$

and similarly,

$$\limsup_{t \rightarrow \infty} N_{mr}(t) = \frac{\sigma_P^*(f)P^\diamond}{\mu_{mr}^* + \epsilon_B C_B \delta_B(1 - u)} = N_{mr}^\diamond$$

Lastly, the human compartment can be shown:

$$\dot{N}_H = \Pi_H - \mu_H N_H(t) - \delta_H I_H(t) \leq \Pi_H - \mu_H N_H(t)$$

This follows that $dN_H/dt < 0$ if $N_H(t) > \Pi_H/\mu_H$. A standard comparison theorem can be used so that $N_H(t) \leq N_H(0)e^{-\mu_H t} + \frac{\Pi_H}{\mu_H}[1 - e^{-\mu_H t}]$. Thus, $N_H \leq \Pi_H/\mu_H$ if $N_H(0) \leq \Pi_H/\mu_H$. Additionally, if $N_H(0) > \Pi_H/\mu_H$, then $N_H(t) \rightarrow \Pi_H/\mu_H$ as $t \rightarrow \infty$. That is, $\limsup_{t \rightarrow \infty} N_H(t) \leq \Pi_H/\mu_H = N_H^\diamond$.

Lemma 1. *All solutions of the model with non-negative initial values remain non-negative and bounded for all $t > 0$.*

Proof. The right side of the equations in the model are continually differentiable and locally-Lipschitz at $t = 0$. From the Picard-Lindelöf theorem, it follows that a unique solution of the model with non-negative initial conditions exists in Ω for all $t > 0$. Since it was assumed that $(1 - \frac{E}{K_E})_+ \geq 0$ for all $t \geq 0$, then $E(t) \leq K_E$ for all $t \geq 0$. Therefore, $E(t) \leq K_E$ for all $t \geq 0$. From the other equations that follow, the solutions of the other state variables from the model are bounded and the solutions of the model are bounded.

Theorem 1. *The region Ω is positively-invariant and attracts all solutions of the model.*

Proof. This result follows from Lemma 1. The invariance of Ω_4 is established from if $E(t) > K_E$, then $\dot{E} < 0$. Also, $\dot{L} < 0$ when $L(t) > L^\diamond(t)$ and $\dot{P} < 0$ when $P(t) > P^\diamond(t)$. Similarly, for both Ω_2 and Ω_3 , $\dot{N}_{vs} < 0$ when $N_{vs}(t) > N_{vs}^\diamond(t)$ and $\dot{N}_{vr} < 0$ when $N_{vr}(t) > N_{vr}^\diamond(t)$. Lastly, for Ω_1 , $\dot{N}_H < 0$ when $N_H(t) > N_H^\diamond(t)$. Hence, the region $\Omega = \Omega_1 \times \Omega_2 \times \Omega_3 \times \Omega_4$ is positively invariant with respect to the model and attracts all positive solutions, since the sub-regions $\Omega_i (i = 1, 2, 3, 4)$ are positively-invariant and attracting with respect to the model, therefore it is sufficient to study the model within this range.

$$\begin{aligned}\Omega_1 &= \left(B_1 \in \mathbb{R}_+^4 : N_H(t) \leq \frac{\Pi_H}{\mu_H} \right) \\ \Omega_2 &= \left(B_2 \in \mathbb{R}_+^3 : N_{ms} \leq N_{ms}^\diamond \right) \\ \Omega_3 &= \left(B_3 \in \mathbb{R}_+^3 : N_{mr} \leq N_{mr}^\diamond \right) \\ \Omega_4 &= \left(B_4 \in \mathbb{R}_+^3 : E_m \leq K_E, L_m \leq L^\diamond, P_m \leq P^\diamond \right)\end{aligned}$$

4.1.2 Existence and Asymptotic Stability of Equilibria

Here the dynamics of the autonomous version of the model are studied where weather-dependant parameters of the model are considered to be constants. It is convenient for the following entomological quantity to be identified, r_0 , which is the net production number which measures the average rate at which new adult female mosquitoes are produced.

$$\begin{aligned}
\dot{E} = 0 &= EFD(M^*) - \frac{EFD(E^*)(M^*)}{K_E} - K_1(E^*) \\
&= K_E EFD(M^*) - \frac{EFD(E^*)(M^*)K_E}{K_E} - K_1(E^*)K_E \\
E^* &= \frac{EFD(M^*)K_E}{K_E K_1 + EFD(M^*)}
\end{aligned}$$

Following the simplification for E^* , the following equations must be solved so that M^* may be substituted to solve for E^* . This is done by using subsequent equation solutions in the following order to write M^* in terms of E^* .

$$\begin{aligned}
L^* &= \frac{\sigma_E(E^*)}{K_2} \\
P^* &= \frac{\sigma_L(L^*)}{K_3} = \frac{\sigma_L \sigma_E(E^*)}{K_2 K_3} \\
M^* &= \frac{q\sigma_P(P^*)}{K_4} = \frac{q\sigma_P \sigma_L \sigma_E(E^*)}{K_2 K_3 K_4}
\end{aligned}$$

where,

$$\begin{aligned}
K_1 &= \sigma_E + \mu_E, K_2 = \sigma_L + \mu_L \\
K_3 &= q\sigma_P + \mu_P, K_4 = \mu_{mr} + \epsilon_B C_B \delta_B (1 - u)
\end{aligned}$$

Now E^* is solved with substitution giving:

$$E^* = \frac{EFD \left(\frac{q\sigma_P\sigma_L\sigma_E(E^*)}{K_2K_3K_4} \right) K_E}{K_1K_E + EFD \left(\frac{q\sigma_P\sigma_L\sigma_E(E^*)}{K_2K_3K_4} \right)}$$

$$K_1K_E + \frac{EFDq\sigma_P\sigma_L\sigma_E(E^*)}{K_2K_3K_4} = \frac{EFDq\sigma_P\sigma_L\sigma_E}{K_2K_3K_4} K_E$$

$$K_1K_2K_3K_4K_E + EFDq\sigma_P\sigma_L\sigma_E(E^*) = EFDq\sigma_P\sigma_L\sigma_E K_E$$

$$E^* = \frac{(EFDq\sigma_P\sigma_L\sigma_E - K_1K_2K_3K_4)K_E}{EFDq\sigma_P\sigma_L\sigma_E}$$

$$E^* = K_E \left(1 - \frac{K_1K_2K_3K_4}{EFDq\sigma_P\sigma_L\sigma_E} \right)$$

Where,

$$r_0 = \frac{EFDq\sigma_P\sigma_L\sigma_E}{K_1K_2K_3K_4}$$

Similarly to the method of inspection described by [29], r_0 can be determined as follows: it is the product of the rate at which the eggs are laid by adult female mosquitoes (EFD), the probability that the eggs survive and hatch into larvae $\left(\frac{\sigma_E}{K_1}\right)$, the probability that the larvae survive and develop into pupae $\left(\frac{\sigma_L}{K_2}\right)$, the probability that the pupae survive and mature into adult female mosquitoes $\left(\frac{q\sigma_P}{K_3}\right)$, and the average lifespan of an adult female mosquito $\left(\frac{1}{K_4}\right)$. The threshold quantity (r_0) is similar to the vectorial reproduction number in [30], for which mosquito population exists whenever $r_0 > 1$ and no mosquito population exists for $r_0 < 1$ at equilibrium.

Now the asymptotic properties of different entomological states and disease presence are explored for understanding model behavior and related thresholds. The autonomous model has:

(i) A trivial disease free equilibrium (DFE) where no mosquitoes exist:

$$\mathcal{T}_1 = (S_H^*, E_H^*, I_H^*, R_H^*, S_{ms}^*, E_{ms}^*, I_{ms}^*, S_{mr}^*, E_{mr}^*, I_{mr}^*, E^*, L^*, P^*) = \left(\frac{\Pi_H}{\mu_H}, 0, 0, 0, 0, 0, 0, 0, 0, 0, 0, 0, 0 \right)$$

(ii) A non-trivial sensitive-only disease-free boundary equilibrium:

$$\mathcal{T}_2 = (S_H^*, 0, 0, 0, S_{ms}^*, 0, 0, 0, 0, 0, E^*, L^*, P^*)$$

$$\text{where, } S_H^* = \frac{\Pi_H}{\mu_H}, S_{ms}^* = \frac{\sigma_P(1-f)P^*}{\mu_{ms} + \epsilon_B C_B \delta_B}, E^* = K_E \left(1 - \frac{1}{r_0} \right), L^* = \frac{\sigma_E E^*}{\sigma_L + \mu_L}, \text{ and } P^* = \frac{\sigma_L L^*}{\sigma_P + \mu_P}.$$

(iii) A non-trivial resistant-only disease-free boundary equilibrium:

$$\mathcal{T}_3 = (S_H^{**}, 0, 0, 0, 0, 0, 0, S_{mr}^{**}, 0, 0, E^{**}, L^{**}, P^{**})$$

$$\text{where, } S_H^{**} = \frac{\Pi_H}{\mu_H}, S_{mr}^{**} = \frac{\sigma_P f P^{**}}{\mu_{mr} + \epsilon_B C_B \delta_B (1-u)}, E^{**} = K_E \left(1 - \frac{1}{r_0} \right), L^{**} = \frac{\sigma_E E^{**}}{\sigma_L + \mu_L}, \text{ and } P^{**} = \frac{\sigma_L L^{**}}{\sigma_P + \mu_P}.$$

(iv) A non-trivial coexistence equilibrium which represents an equilibrium where the component of each state variable of the model is nonzero:

$$\mathcal{T}_4 = (S_H^{***}, E_H^{***}, I_H^{***}, R_H^{***}, S_{ms}^{***}, E_{ms}^{***}, I_{ms}^{***}, S_{mr}^{***}, E_{mr}^{***}, I_{mr}^{***}, E^{***}, L^{***}, P^{***})$$

The next generation operator method can be used to analyze the local asymptotic stability of the DFE [11]. The associated matrix F (new infection terms) and matrix V (linear transition terms) are given, respectively, by:

$$F = \begin{bmatrix} 0 & 0 & 0 & 0 & 0 & \frac{\beta_{Hms} S_{ms}^*}{N_H^*} \\ 0 & 0 & 0 & 0 & 0 & 0 \\ 0 & 0 & 0 & 0 & 0 & \frac{\beta_{Hmr} S_{mr}^*}{N_H^*} \\ 0 & 0 & 0 & 0 & 0 & 0 \\ 0 & \frac{\beta_{msH} S_H^*}{N_H^*} & 0 & \frac{\beta_{mrH} S_H^*}{N_H^*} & 0 & 0 \\ 0 & 0 & 0 & 0 & 0 & 0 \end{bmatrix} \begin{bmatrix} E_{ms} \\ I_{ms} \\ E_{mr} \\ I_{mr} \\ E_H \\ I_H \end{bmatrix}$$

and,

$$V = \begin{bmatrix} \sigma_{ms} + \mu_{ms} & 0 & 0 & 0 & 0 & 0 \\ -\sigma_{ms} & \mu_{ms} & 0 & 0 & 0 & 0 \\ 0 & 0 & \sigma_{mr} + \mu_{mr} & 0 & 0 & 0 \\ 0 & 0 & -\sigma_{mr} & \mu_{mr} & 0 & 0 \\ 0 & 0 & 0 & 0 & \sigma_H + \mu_H & 0 \\ 0 & 0 & 0 & 0 & -\sigma_H & \gamma_H + \delta_H + \mu_H \end{bmatrix} \begin{bmatrix} E_{ms} \\ I_{ms} \\ E_{mr} \\ I_{mr} \\ E_H \\ I_H \end{bmatrix}$$

The reproduction number (\mathcal{R}_0) of the model which considers the absence of all insecticide-based interventions which in this model is only insecticide treated bed nets, is given by:

$$\mathcal{R}_0 = \rho(FV^{-1})$$

which gives,

$$\begin{aligned} \mathcal{R}_0 &= \sqrt{\mathcal{R}_{0ms} + \mathcal{R}_{0mr}} \\ &= \sqrt{(\mathcal{R}_{0msH} \times \mathcal{R}_{0Hms}) + (\mathcal{R}_{0mrH} \times \mathcal{R}_{0Hmr})} \end{aligned}$$

It is assumed in the model that the transmission rates between sensitive and resistant mosquito classes are equal where $\beta_{msH} = \beta_{mrH}$ and $\beta_{Hms} = \beta_{Hmr}$, thus are denoted as β_{mH} and β_{Hm} , respectively. Additionally, $\mu_{mr} = \mu_{ms}$ and $\sigma_{mr} = \sigma_{ms}$, thus are denoted as μ_m and σ_m , respectively. Each of the constituent \mathcal{R} values at DFE are solved as,

$$\begin{aligned} \mathcal{R}_{msH} &= \mathcal{R}_{mrH} = \frac{\beta_{mH} S_H^* \sigma_H}{N_H^* (\sigma_H + \mu_H) (\gamma_H + \mu_H + \delta_H)} \\ \mathcal{R}_{Hms} &= \frac{\beta_{Hm} S_m^* \sigma_m}{N_H^* (\sigma_m + \mu_m) \mu_m} \\ \mathcal{R}_{Hmr} &= \frac{\beta_{Hm} S_m^* \sigma_m}{N_H^* (\sigma_m + \mu_m) \mu_m} \end{aligned}$$

Also note for the DFE conditions,

$$\begin{aligned} S_{ms}^* &= \frac{\sigma_P (1-f) P^*}{\mu_m} \\ S_{mr}^* &= \frac{\sigma_P (f) P^*}{\mu_m} \end{aligned}$$

The value \mathcal{R}_C which is similar to \mathcal{R}_0 (although also contains bed net coverage) is given as:

$$\mathcal{R}_C = \sqrt{(\mathcal{R}_{C_{msH}} \times \mathcal{R}_{CH_{ms}}) + (\mathcal{R}_{C_{mrH}} \times \mathcal{R}_{CH_{mr}})}$$

but now with each of the constituent \mathcal{R} values solved as,

$$\begin{aligned}\mathcal{R}_{msH} = \mathcal{R}_{mrH} &= \frac{(1 - \epsilon_B C_B) \beta_{mH} S_H^* \sigma_H}{N_H^* (\sigma_H + \mu_H) (\gamma_H + \mu_H + \delta_H)} \\ \mathcal{R}_{Hms} &= \frac{\beta_{Hm} S_{ms}^* \sigma_m}{N_H^* (\sigma_m + \mu_m + \epsilon_B C_B \delta_B) (\mu_m + \epsilon_B C_B \delta_B)} \\ \mathcal{R}_{Hmr} &= \frac{\beta_{Hm} S_{mr}^* \sigma_m}{N_H^* (\sigma_m + \mu_m + \epsilon_B C_B \delta_B) (\mu_m + \epsilon_B C_B \delta_B)}\end{aligned}$$

where for the DFE conditions,

$$S_{ms}^* = \frac{\sigma_P (1 - f) P^*}{\mu_m + \epsilon_B C_B \delta_B} \quad S_{mr}^* = \frac{\sigma_P (f) P^*}{\mu_m + \epsilon_B C_B \delta_B (1 - u)}$$

The results below follows from Theorem 2 in [11].

Lemma 2: *The trivial disease free equilibrium is locally-asymptotically stable if $\mathcal{R}_0(\mathcal{R}_C) < 1$, and unstable if $\mathcal{R}_0(\mathcal{R}_C) > 1$.*

The \mathcal{R}_0 of the model is the geometric mean of the reproduction numbers for human-to-mosquito ($\mathcal{R}_{0, HM}$, $\mathcal{R}_{C, HM}$) and mosquito-to-human ($\mathcal{R}_{0, MH}$, $\mathcal{R}_{C, MH}$) transmission interactions. Due to two generations being required to complete the human-vector-human or vector-human-vector malaria transmission cycle, the geometric mean is present. The general epidemiological implication of this lemma is that a small influx of infected mosquitoes would not generate a large outbreak when \mathcal{R}_0 is less than unity and the disease would die out over time. Although, this may not always be the case due to backwards bifurcation as explored in [31].

As mentioned by [26], it can be shown using the next generation operator method that the associated reproduction number of the autonomous model is given by:

$$\mathcal{R}_{0ms} = \sqrt{\mathcal{R}_{Hms} \times \mathcal{R}_{msH}}$$

and,

$$\mathcal{R}_{0mr} = \sqrt{\mathcal{R}_{Hmr} \times \mathcal{R}_{mrH}}$$

where separate calculations done by inspection for \mathcal{R}_{0ms} and \mathcal{R}_{0mr} shows, respectively:

$$\mathcal{R}_{msH} = (1 - \epsilon_B C_B) \beta_{msH} \left(\frac{\sigma_H}{\sigma_H + \mu_H} \right) \left(\frac{1}{\gamma_H + \mu_H + \delta_H} \right)$$

$$\mathcal{R}_{Hms} = \left(\frac{\beta_{HM} S_{ms}^*}{N_H^*} \right) \left(\frac{\sigma_{ms}}{\sigma_{ms} + \mu_{ms} + \epsilon_B C_B \delta_B} \right)$$

and,

$$\mathcal{R}_{mrH} = (1 - \epsilon_B C_B) \beta_{mrH} \left(\frac{\sigma_H}{\sigma_H + \mu_H} \right) \left(\frac{1}{\gamma_H + \mu_H + \delta_H} \right)$$

$$\mathcal{R}_{Hmr} = \left(\frac{\beta_{HM} S_{mr}^*}{N_H^*} \right) \left(\frac{\sigma_{mr}}{\sigma_{mr} + \mu_{mr} + \epsilon_B C_B \delta_B (1 - u)} \right)$$

thus giving the results:

$$\mathcal{R}_{0ms} = \sqrt{\frac{(1 - \epsilon_B C_B) \beta_{msH} \sigma_H \beta_{HM} S_{ms}^* \sigma_{ms}}{(\sigma_H + \mu_H)(\gamma_H + \mu_H + \delta_H) N_H^* (\sigma_{ms} + \mu_{ms} + \epsilon_B C_B \delta_B)}}$$

and,

$$\mathcal{R}_{0mr} = \sqrt{\frac{(1 - \epsilon_B C_B) \beta_{mrH} \sigma_H \beta_{HM} S_{mr}^* \sigma_{mr}}{(\sigma_H + \mu_H)(\gamma_H + \mu_H + \delta_H) N_H^* [\sigma_{mr} + \mu_{mr} + \epsilon_B C_B \delta_B (1 - u)]}}$$

Theorem 2: Relating to the competitive-exclusion principle, the sensitive-only (resistant-only) boundary equilibrium is locally-asymptotically stable if $\mathcal{R}_{0ms}(\mathcal{R}_{0mr}) > 1$ and $\mathcal{R}_{0mr}(\mathcal{R}_{0ms}) < 1$.

Conjecture 1: The model has a non-trivial coexistence equilibrium where all the states are nonzero which locally-asymptotically stable whenever $\min\{\mathcal{R}_{0ms}, \mathcal{R}_{0mr}\} \geq 1$.

4.2 Application results

Discussion and Conclusion

We have presented a practical and important tool for preventing additional malaria cases through a web and mobile application. As malaria cases continue to cause hundreds of thousands of deaths annually, this application is vital in helping reduce those numbers. Used in combination with other preventive measures, such as LLINs and ITNs, the application is highly effective in helping prevent new cases. Insecticide resistance is also important to consider since it affects transmission rates, thus the application considers resistance in the mathematical model. Lastly, the application is user-friendly (simple to use and requires minimal interpretation from the user) and accessible to many (available in multiple languages).

In this study, adult mosquitoes and humans are given an SEI and SEIR model respectively in order to properly observe transmission. Both adult mosquitoes and humans are susceptible to malaria. In addition, they both go through an exposed stage before becoming infectious. However, it is assumed that adult mosquitoes do not recover from malaria in contrast to humans. Bed net usage is also taken into consideration in the adult mosquito and human dynamics because it affects the rate of transmission.

Although immature mosquitoes cannot transmit malaria, they are an essential component in the math model. Without it, there could possibly be overestimation or underestimation of malaria burden [9]. As pupae mature into adults and adults reproduce to lay eggs, it is evident that immature and adult mosquitoes cannot be independently observed. The parameters in the immature stage are mostly temperature dependent, and since the adult dynamics is highly dependent on the immature stage and the human dynamics is highly dependent on adult mosquitoes, the overall model is dependent on the temperature. Temperature values for these parameters are obtained through a particular parameter in the immature dynamic, carrying capacity (K_E), is dependent on precipitation since mosquitoes lay their eggs in bodies of water. The carrying capacity of eggs determines the maximum number of eggs to be laid in a particular region, which in turn determines the number of adult mosquitoes in that region. Therefore, carrying capacity has an indirect effect on the rate of transmission.

Using some values from the differential equations of the mosquito and human dynamics, the entomological inoculation rate (EIR) calculates the risk of infection. That result is evaluated and then translated into a sim-

ple, user-friendly message, notifying the user of whether he or she is in a high or low risk region. Another way to determine risk is calculating the basic reproduction number (R_0). Ideally, EIR and R_0 would both be used as additional tools for determining an individual's risk. Unfortunately, due to its complexity, R_0 's results were impractical. Thus only EIR was used to determine risk of infection.

Analysis of the model proves that the parameters are realistic. The eggs per female mosquito per day (EFD) increases between 15 – 27 degrees Celsius. The immature stage development rate also increases starting at 15 degrees Celsius but continues to increase until 30 degrees Celsius. The rate of becoming infectious for adults also falls into this range. The adult stage death rate is extremely low until it reaches around 38 degrees Celsius, where it drastically increases. The transmission rate increases after 15 degrees Celsius then is expected to cut off after 40 degrees Celsius with the assumption that adult mosquitoes would have died off by then. This all compliments the fact that malaria burden increases when temperatures are in the range of 16-28 degrees Celsius [9].

The work presented in this paper provides a means of predicting an individual's risk of contracting malaria in a particular region. Such a prediction is vital in combating the spread of malaria because it can prevent an individual from traveling to a high-risk area, or it could encourage the individual to take protective measures, such as sleeping under a bed net or taking anti-malarial drugs before traveling. The differential equations in the mathematical model monitor possible transmission by calculating the number of immature mosquitoes, potential infectious adult mosquitoes, and infected humans in each region. The results from the differential equations provide the necessary values for calculating EIR, which will calculate the user's risk. The intention is to format this early warning system as a mobile application and a website so the public can have access to it and stay informed.

The weather components including temperature and rainfall used in the model were integrated based on the previous work of other authors who fit parameters from fitting data sets with consideration of other models. Given the spatial differences that can affect malaria transmission dynamics, the model's accuracy can be further improved with the availability of specific regional data with calculations that can be performed on a large scale for fitting parameters. Alternative models should also be taken into consideration such as the agent-based modeling approaches [24][25] that

emphasize weather effects on malaria incidence.

We could have worked with HydroSheds data to better inform the carrying capacity parameter for eggs in the aquatic stage. The weather data could have been more accurate as well, since historical weather data for more than a year was available through the API, granted we had a paid subscription. There are many such possibilities for improving upon the model we have used in this application, as well as the early warning system as a whole. Our main goal was to take the first step in creating an actual product, since to our knowledge, no one has attempted to do anything similar. We hope it will encourage others to adapt our model and build upon it, with the vision of eradicating malaria.

Acknowledgments

We would like to thank Dr. Fabio Milner, Director of the Simon A. Levin Mathematical, Computational and Modeling Sciences Center (Levin Center), for giving us the opportunity to participate in the Quantitative Research in the Life and Social Sciences program. We would also like to thank Co-Directors Dr. Abba Gumel and Dr. John Nagy for their efforts in planning and executing the program's instruction and activities. We also recognize the work of the many administrative staff and tutors who supported this effort. This research was conducted as part of 2022 QRLSSP at the Levin Center (MCMSC) at Arizona State University (ASU). This project has been partially supported by grants from the National Science Foundation (NSF Grant-DMS-1757968 and NSF Grant FAIN-2150492), the National Security Agency (NSA Grant H98230-20-1-0164), the Office of the President of ASU, and the Office of the Provost of ASU. We are especially grateful to Dr. Abba Gumel and Dr. Steffen Eikenberry for their guidance, as well as Hovig Artinian, Theophilus Kwofie, and Jordy Rodriguez for their support, throughout the research.

References

- [1] Geneva: World Health Organization. (2021). World malaria report 2021. World Health Organization.
- [2] Carter, R., & Mendis, K. N. (2002). Evolutionary and historical aspects of the burden of malaria. *Clinical microbiology reviews*, 15(4), 564–594. <https://doi.org/10.1128/CMR.15.4.564-594.2002>

- [3] Antinori, S., Galimberti, L., Milazzo, L., & Corbellino, M. (2012). Biology of human malaria plasmodia including *Plasmodium knowlesi*. *Mediterranean journal of hematology and infectious diseases*, 4(1), e2012013. <https://doi.org/10.4084/MJHID.2012.013>
- [4] Gallup, J., & Sachs, J. (2001). The economic burden of malaria, *The American Journal of Tropical Medicine and Hygiene* Am J Trop Med Hyg, 64(1_suppl). https://www.ajtmh.org/view/journals/tpmd/64/1_suppl/article-p85.xml
- [5] Binka, F. N., Indome, F., & Smith, T. (1998). Impact of spatial distribution of permethrin-impregnated bed nets on child mortality in rural northern Ghana., *The American journal of tropical medicine and hygiene*, 59(1), 80-85. <https://www.ajtmh.org/view/journals/tpmd/59/1/article-p80.xml>
- [6] Centers for Disease Control and Prevention. (2021, December 16). CDC - Malaria - malaria worldwide - impact of malaria. Centers for Disease Control and Prevention. Retrieved from https://www.cdc.gov/malaria/malaria_worldwide/impact.html
- [7] Mohammed-Awel, J., & Gumel, A. B. (2019). Mathematics of an epidemiology-genetics model for assessing the role of insecticides resistance on malaria transmission dynamics. *Mathematical Biosciences*, 312, 33-49. <https://www-sciencedirect-com.ezproxy1.lib.asu.edu/science/article/pii/S0025556417306636#fig0001>
- [8] Amoah, B., McCann, R. S., Kabaghe, A. N., Mburu, M., Chipeta, M. G., Moraga, P., Gowelo, S., Tizifa, T., van den Berg, H., Mzilahowa, T., Takken, W., van Vugt, M., Phiri, K. S., Diggle, P. J., Terlouw, D. J., & Giorgi, E. (2021). Identifying *Plasmodium falciparum* transmission patterns through parasite prevalence and entomological inoculation rate. *eLife*, 10, e65682. <https://doi.org/10.7554/eLife.65682>
- [9] Agosto, F. B., Gumel, A. B., & Parham, P. E. (2015). Qualitative assessment of the role of temperature variations on malaria transmission dynamics. *Journal of Biological Systems*, 23(04), 1550030. <https://www.worldscientific.com/doi/abs/10.1142/s0218339015500308>
- [10] Enahoro, I., Eikenberry, S., Gumel, A. B., Huijben, S., & Paaijmans, K. (2020). Long-lasting insecticidal nets and the quest for malaria eradication: a mathematical modeling approach. *Journal of Mathematical Biology*, 81(1), 113-158. <https://link.springer.com/article/10.1007/s00285-020-01503-z>

- [11] van den Driessche, P., & Watmough, J. (2002). Reproduction numbers and sub-threshold endemic equilibria for compartmental models of disease transmission. *Mathematical biosciences*, 180(1-2), 29-48. <https://www.sciencedirect.com/science/article/pii/S0025556402001086>
- [12] Smith, M. L., & Styczynski, M. P. (2018). Systems Biology-Based Investigation of Host-Plasmodium Interactions. *Trends in parasitology*, 34(7), 617-632. <https://doi.org/10.1016/j.pt.2018.04.003>
- [13] Anickode, A. (2020). Using Mathematics to Assess the Impact of Insecticide-based Interventions and Vaccination on Malaria Control. *Society for Industrial and Applied Mathematics*. <https://www.siam.org/Portals/0/Publications/SIURO/Vol13/S131494.pdf?ver=2020-08-03-123911-783>
- [14] Eikenberry, S.E., Gumel, A.B. (2018). Mathematical modeling of climate change and malaria transmission dynamics: a historical review. *J. Math. Biol.* 77, 857-933. <https://doi.org/10.1007/s00285-018-1229-7>
- [15] Eikenberry, S.E., Gumel, A.B. (2019). Mathematics of Malaria and Climate Change. In: Kaper, H., Roberts, F. (eds) *Mathematics of Planet Earth*. *Mathematics of Planet Earth*, vol 5. Springer, Cham. https://doi.org/10.1007/978-3-030-22044-0_4
- [16] Vestergaard, KEMRI-CGHR, ESRI Eastern Africa. (n.d.). IRMapper: Anopheles. Retrieved from <https://anopheles.irmapper.com/>
- [17] Mohammed-Awel, J., Iboi, E. A., & Gumel, A. B. (2020). Insecticide resistance and malaria control: A genetics-epidemiology modeling approach. *Mathematical biosciences*, 325, 108368. <https://doi.org/10.1016/j.mbs.2020.108368>
- [18] Smith, D. L., Battle, K. E., Hay, S. I., Barker, C. M., Scott, T. W., & McKenzie, F. E. (2012). Ross, macdonald, and a theory for the dynamics and control of mosquito-transmitted pathogens. *PLoS pathogens*, 8(4), e1002588. <https://doi.org/10.1371/journal.ppat.1002588>
- [19] Lysenko, A., & Semashko, I. (1968). *Geography of malaria. a medical-geographical study of an ancient disease.*
- [20] Baton, L. A., & Ranford-Cartwright, L. C. (2005). Spreading the seeds of million-murdering death: metamorphoses of malaria in the mosquito. *Trends in parasitology*, 21(12), 573-580. <https://doi.org/10.1016/j.pt.2005.09.012>

- [21] White, M. T., Griffin, J. T., Churcher, T. S., Ferguson, N. M., Basáñez, M. G., & Ghani, A. C. (2011). Modelling the impact of vector control interventions on *Anopheles gambiae* population dynamics. *Parasites & vectors*, 4(153). <https://doi.org/10.1186/1756-3305-4-153>
- [22] Centers for Disease Control and Prevention. (2022). Where malaria occurs. Centers for Disease Control and Prevention. <https://www.cdc.gov/malaria/about/distribution.html>
- [23] Hemingway, J., Ranson, H., Magill, A., Kolaczinski, J., Fornadel, C., Gimnig, J., Coetzee, M., Simard, F., Roch, D. K., Hinzoumbe, C. K., Pickett, J., Schellenberg, D., Gething, P., Hoppé, M., & Hamon, N. (2016). Averting a malaria disaster: will insecticide resistance derail malaria control?. *Lancet* (London, England), 387(10029), 1785–1788. [https://doi.org/10.1016/S0140-6736\(15\)00417-1](https://doi.org/10.1016/S0140-6736(15)00417-1)
- [24] Weidong Gu, Gerry F. Killeen, Charles M. Mbogo, James L. Regens, John I. Githure, & John C. Beier. (2003). An individual-based model of *Plasmodium falciparum* malaria transmission on the coast of Kenya, *Transactions of The Royal Society of Tropical Medicine and Hygiene*, 97(1), 43–50. [https://doi.org/10.1016/S0035-9203\(03\)90018-6](https://doi.org/10.1016/S0035-9203(03)90018-6)
- [25] Hoshen, M. B., & Morse, A. P. (2004). A weather-driven model of malaria transmission. *Malaria journal*, 3, 32. <https://doi.org/10.1186/1475-2875-3-32>
- [26] Kamaldeen Okuneye, Steffen E. Eikenberry & Abba B. Gumel. (2019). Weather-driven malaria transmission model with gonotrophic and sporogonic cycles. *Journal of Biological Dynamics*, 13, 288-324. <https://doi.org/10.1080/17513758.2019.1570363>
- [27] Grover-Kopec, E., Kawano, M., Klaver, R. W., Blumenthal, B., Ceccato, P., Connor, S. J. (2005). An online operational rainfall-monitoring resource for epidemic malaria early warning systems in Africa. *Malaria Journal*, 4(1), 1-5. <https://link.springer.com/article/10.1186/1475-2875-4-6>
- [28] Malaria early warning system. Climate Data Library. (n.d.). Retrieved July 15, 2022, from <https://iridl.ldeo.columbia.edu/maproom/Health/Regional/Africa/Malaria/System.html>
- [29] Brozak, S. J., Mohammed-Awel, J., & Gumel, A. B. (2022). Mathematics of a single-locus model for assessing the impacts of pyrethroid resistance and temperature on population abundance of malaria mosquitoes. *Infectious Disease Modelling*, 7(3), 277–316. <https://doi.org/10.1016/j.idm.2022.05.007>

- [30] Okuneye, K., Abdelrazec, A., Gumel, A. B. (2018). Mathematical analysis of a weather-driven model for the population ecology of mosquitoes. *Mathematical biosciences and engineering : MBE*, 15(1), 57–93. <https://doi.org/10.3934/mbe.2018003>
- [31] Garba, S. M., Gumel, A. B., Abu Bakar, M. R. (2008). Backward bifurcations in dengue transmission dynamics. *Mathematical biosciences*, 215(1), 11–25. <https://doi.org/10.1016/j.mbs.2008.05.002>
- [32] Beck-Johnson, L. M., Nelson, W. A., Paaijmans, K. P., Read, A. F., Thomas, M. B., Bjørnstad, O. N. (2013). The effect of temperature on *Anopheles* mosquito population dynamics and the potential for malaria transmission. *PloS one*, 8(11). <https://doi.org/10.1371/journal.pone.0079276>
- [33] Parham, P. E., Michael, E. (2010). Modeling the effects of weather and climate change on malaria transmission. *Environmental health perspectives*, 118(5), 620–626. <https://doi.org/10.1289/ehp.0901256>
- [34] Bhatt, S., Weiss, D. J., Cameron, E., Bisanzio, D., Mappin, B., Dalrymple, U., Battle, K., Moyes, C. L., Henry, A., Eckhoff, P. A., Wenger, E. A., Briët, O., Penny, M. A., Smith, T. A., Bennett, A., Yukich, J., Eisele, T. P., Griffin, J. T., Fergus, C. A., Lynch, M., ... Gething, P. W. (2015). The effect of malaria control on *Plasmodium falciparum* in Africa between 2000 and 2015. *Nature*, 526(7572), 207–211. <https://doi.org/10.1038/nature15535>